

EPC GaN Transistor Application Readiness: Phase Three Testing



Yanping Ma, PhD, Director of Quality and Reliability, Efficient Power Conversion Corporation

Efficient Power Conversion Corporation's (EPC) enhancement mode Gallium Nitride (eGaN®) power transistors, although similar to standard power MOSFETs, deliver performance unattainable by silicon-based devices. EPC power transistors offer standard power converter topologies added performance and improved efficiency while maintaining the simplicity of older designs. EPC's risk-reduction results to date include the placement of over 810 devices, at their maximum operating ratings, in a wide variety of stress tests. Over 960,000 total device hours of reliability testing validates the readiness of eGaN transistors to supplant their silicon counter-parts for power switching applications.

Reliability Test Results Overview

The key reliability considerations for power transistors include: (a) device stability in the on-state when the transistor is fully enhanced with voltage applied on the gate; (b) device stability in the off-state when the transistor is in voltage blocking mode withstanding up to its rated drain-source voltage; and (c) device stability in switching operation. Device stability is impacted by device design, packaging technology, and operating environment. Good reliability results, based on millions of device hours under stress, have been reported for depletion mode GaN HEMTs (high electron mobility transistors) for RF applications¹⁻³ and power switching applications⁴.

In June 2009, Efficient Power Conversion Corporation introduced the first enhancement mode Gallium Nitride on silicon power transistors designed specifically as replacements for power MOSFETs⁵. These high electron mobility transistors were subjected to a wide variety of stress tests under conditions that are typical for power MOSFET used in switch mode power conversion. These tests included:

- Stability under drain-source bias whereby parts were subjected to a drain-source voltage equal to the maximum rated voltage at the maximum rated temperature (high temperature reverse bias, or HTRB)
- Stability under gate-source bias whereby devices were subjected to gate-source

voltages at the maximum rated temperature (high temperature gate bias, or HTGB)

- Temperature cycling (TC)
- Temperature and humidity, with bias from drain to source (THB)
- Moisture sensitivity level (MSL) classification
- Operating life whereby parts were assembled onto power supply boards and subjected to actual DC-DC conversion operating conditions

Reliability test results are summarized in Table I, in which the type of test, stress conditions, part numbers, sample size, stress hours, and number of fails are listed. JEDEC standards were followed when applicable.

Parts were mounted on FR408 adaptor cards (unless otherwise stated) and electrical parameters were measured at time zero. Interim readout points were all at room temperature. The underfill material used, where applicable, was Loctite FP4549Si.

As seen in Table I, the eGaN transistor has demonstrated excellent reliability. At the time of this writing over 810 parts were stressed for over 960,000 device hours of reliability testing with no failures. Over the entire stress period device electrical parameters remained stable.

Several reliability issues with non-commercial GaN devices have been reported in the literature. Two major issues are current collapse (dynamic $R_{DS(on)}$)⁶⁻¹⁷ and gate leakage degradation¹⁸⁻²¹. EPC's eGaN products were subjected to a wide variety of stress tests to validate they functioned reliably under accelerated stress conditions and did not display noteworthy degradation as a result of the mechanisms reported in the academic literature.

Dynamic $R_{DS(on)}$

Dynamic $R_{DS(on)}$, also known as "current collapse", is a phenomenon whereby the drain current decreases as a result of electron trapping near the channel region (see the schematic of a GaN HEMT structure in Figure 1). The magnitude of "current collapse" is strongly dependent on the electric field at the gate-edge where electrons can be accelerated⁶. Electrons may be trapped in the AlGaN/dielectric interface where they charge up the surface states which then act as a virtual gate electrode. This can result in a reversible degradation of drain current⁷. Electrons can also be trapped in the AlGaN barrier layer itself or in the GaN buffer layer below. These high energy electrons can also generate traps, further promoting charge trapping. The high

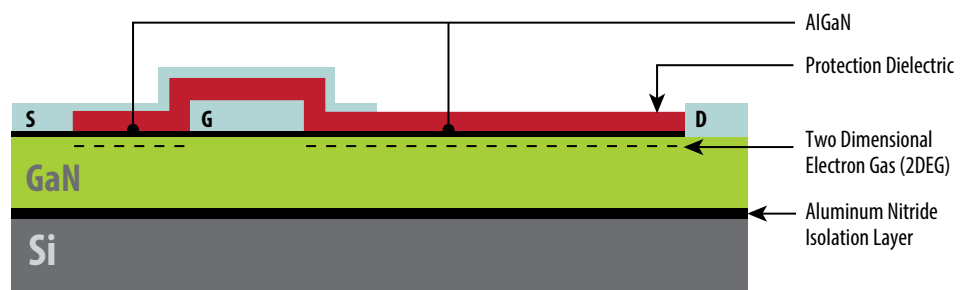


Figure 1. EPC's eGaN transistor structure (not to scale)

electric field could also result in mechanical defects due to the inverse-piezoelectric effect, forming electrically active deep levels that trap electrons and cause a reduction of intrinsic carrier concentrations and the maximum drain current^{8,9}. The crystallographic defects and strain relaxation also lower the electron density in the region next to gate, thereby reducing the current carrying capability¹⁰.

Device design improvements using gate and source field plates are an effective way to reduce the electric field thereby suppressing the increase in on-state resistance as well as gate-leakage degradation^{6,11}. Surface passivation, or surface treatments, can also be effective at reducing the surface trap density and thereby reducing hot-electron degradation²⁻¹³. The use of a conducting substrate acting as a backside field plate helps to mitigate electron trapping in the buffer region beneath the channel⁶. In addition, better confinement of electrons in the potential well and overall improvement in the material quality of AlGaIn/GaN epitaxial layers are important to combat dynamic $R_{DS(on)}$ ¹⁴⁻¹⁶.

EPC has taken steps in material growth, device design, and process optimization to minimize the potential device degradation mechanisms²².

Figure 2 is an illustration of $R_{DS(on)}$ over stress time of EPC1010 with the maximum drain-source voltage applied at an elevated temperature of 150°C (HTRB). Fifty EPC1010 devices were drain biased at 200 V in the stress chamber with gate and source shorted to ground. Device parameters were measured initially at time zero and at each interim readout point. The normalized $R_{DS(on)}$ is the ratio of the post test value over the initial value for each device at each interim readout point. $R_{DS(on)}$ was measured with 5 V on the gate and the source at ground potential. As can be seen, $R_{DS(on)}$ stayed stable over the stress period of 3000 hours. As with EPC1010, a 200 V eGaN transistor, minimal $R_{DS(on)}$ variation was observed on parts from 100 V (EPC1001) and 40 V (EPC1014) eGaN transistors on HTRB when biased with the rated drain-source voltage at an elevated temperature of 125°C.

The stability under gate bias is illustrated in Figure 3 where the normalized $R_{DS(on)}$ is plotted against the stress time. Forty five EPC1001 devices were gate biased at 5V at 125°C in the stress chamber with drain and source shorted to ground (HTGB). Some devices showed $R_{DS(on)}$ shift of about 20% relative to the initial electrical values at the beginning of the test but stayed stable over the stress period of 3000 hours.

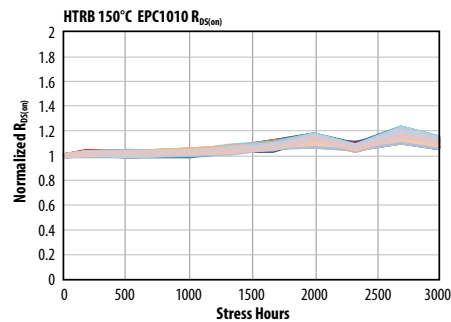


Figure 2. EPC1010 devices were stressed with 200 V applied on the drain in the stress chamber at 150°C, source and gate shorted to ground. $R_{DS(on)}$ was measured with 5 V on the gate at 25°C.

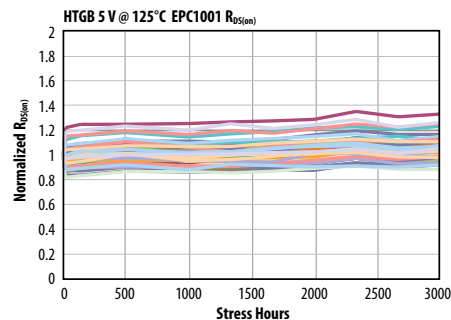


Figure 3. EPC1001 devices were stressed with 5 V on the gate in the stress chamber at 125°C, drain and source shorted to ground. $R_{DS(on)}$ was measured with 5 V on the gate at 25°C.

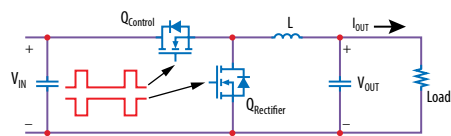
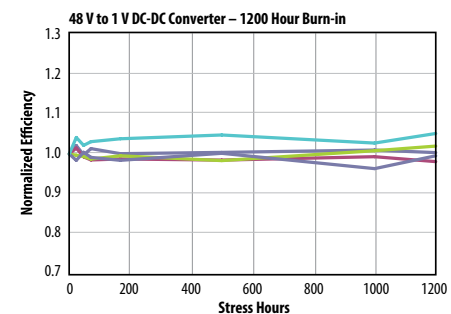


Figure 4. Power supply life test using EPC1001 at 30°C and 10 A. The normalized converter efficiency was plotted over 1200 hours of operating life in (a), and the power supply test circuit was shown in (b).

To test reliability under typical high-stress operating conditions, including the stability of $R_{DS(on)}$, EPC built 48 V – 1 V power supply boards using a “buck converter” topology (see Figure 4(b)). For the burn-in test, EPC1001 (100 V, 7 mΩ) transistors were used for both the control transistor and rectifier switches. This kind of a test is par-

ticularly useful because, in a standard “buck” topology DC-DC converter operating at the high V_{IN}/V_{OUT} ratio of 48 V : 1 V, the control transistor is turned ON with a very low duty cycle (~2%). Conversely, the rectifier transistor is turned ON with a very high duty cycle (~98%). This test therefore stresses devices both at high drain-source voltage and high drain current under actual, fast-switching conditions. The converter was operated at 48 V input voltage, 1 V output voltage, 10 A output current, and at a switching frequency of 250 kHz. The circuit efficiency was measured at time-zero hour, 24, 48, 72, 168, 500, 1000, and 1200 hours. The normalized efficiency vs. burn-in hours (Figure 4(a)) stayed virtually unchanged over the entire burn-in period.

The dynamic $R_{DS(on)}$ phenomenon is not only accelerated by the electric field, but also when both channel current and a high electric field are present in the device¹⁷. The constant conversion efficiency demonstrated in the power supply operation life test indicated that there was no obvious $R_{DS(on)}$ degradation in EPC eGaN transistors under high electric field in the OFF-state, or high channel current in the ON-state, or during switching when both high electric field and high current exist simultaneously.

Recognizing the importance of minimizing the dynamic $R_{DS(on)}$, and committed to continuous design and process improvement, EPC is working to further improve this characteristic.

Gate Leakage Stability

Documented gate leakage degradation mechanisms include inverse-piezoelectric effect¹⁸⁻¹⁹, carrier traps generated by high energy electrons²⁰, and Schottky contact degradation²¹. EPC’s eGaN transistors do not use a Schottky gate and therefore are not vulnerable to this last mechanism.

GaN HEMTs are predicated on the piezoelectric properties of the material in conjunction with spontaneous polarization. The electric field generated between AlGaIn and GaN as a result of strain caused by the lattice mismatch allows high electron channel densities to form at the AlGaIn/GaN interface. High electric fields at the gate edge under drain bias can increase the strain (inverse piezoelectric effect) and therefore affect device reliability. The inverse piezoelectric effect theory has been proposed to explain failure modes that could not be explained by hot-electron injection. In this theory, high electric fields increase the strain in the AlGaIn barrier layer. When a critical drain-

gate voltage is reached, crystallographic defect formation occurs¹⁸⁻¹⁹. These crystallographic defects act as deep level traps assisting electron tunneling, therefore significantly increasing the gate leakage current.

Another proposed mechanism is related to electron initiated impact ionization near the gate edge in the off-state under high drain-gate bias. Electrons tunneling through the AlGa_N barrier create hot holes with energies adequate to inject back into the AlGa_N barrier. These holes may recombine with the trapped electrons releasing energy to produce bulk and transition-layer tunnel traps and interface states²⁰.

To verify the EPC eGa_N transistors do not suffer from these degradation mechanisms, EPC subjected hundreds of parts to high drain bias tests. Figure 5 is an illustration of the gate leakage performance of EPC1010 with 200 V applied on the drain, gate and source shorted to ground (HTRB). The gate leakage (I_{GSS}) was measured with 5 V on the gate and with the drain and source shorted to ground. No gate leakage degradation was observed over the stress period of 3000 hours. As with EPC1010, no gate leakage degradation was observed over the stress period for the 100 V (EPC1001) and 40 V (EPC1014) transistors in the HTRB tests with the max rated drain-source bias applied.

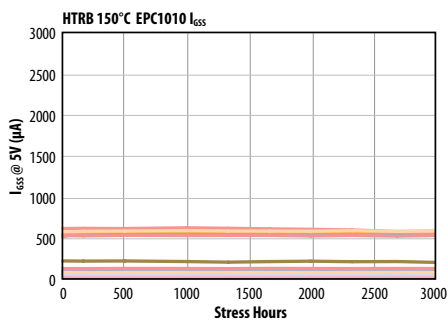


Figure 5. EPC1010 devices were stressed with 200 V applied on the drain in the burn-in chamber at 150°C, source and gate shorted to ground. The gate leakage was measured with 5 V on the gate with drain and source shorted to ground at 25°C.

Stability under Gate Stress

Device stability under gate stress was evaluated by subjecting parts to high temperature gate bias (HTGB) at an elevated temperature of 125°C. Figure 6 is an illustration of the gate leakage in the gate stress test where 5 V was applied on the gate in the stress chamber with drain and sources shorted to ground. As shown in Figure 6 the leakage current stayed stable

and no leakage degradation was observed. The same part number was also subjected to a higher stress with 5.4 V on the gate at 125°C. As with the gate stress test with 5 V on the gate, the gate leakage was stable over the entire stress period of 3000 hours.

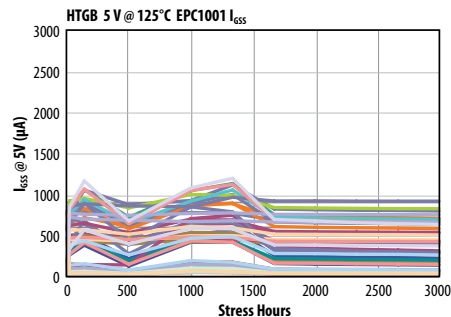


Figure 6. EPC1001 devices were stressed with 5 V on the gate in the burn-in chamber at 125°C, drain and source shorted to ground. The gate leakage was measured with 5 V on the gate with drain and source shorted to ground at 25°C.

Users should avoid subjecting parts to more than 6 V in operation until further improvement on gate rating is made. Transistors subjected to a gate bias greater than 6 V showed stable gate leakage, but began to show increase in the drain-to-source leakage.

EPC recognizes this weakness and is working toward improving the gate maximum voltage rating.

Humidity Sensitivity

EPC's eGa_N transistors are lateral devices with all three terminals: gate, drain, and source on the front side of the chip. The active device is fully encapsulated by passivation layers on the front side as shown in Figure 7. This configuration allows EPC's eGa_N transistors to be used as bare die without additional packaging. The advantages of eliminating plastic packages include elimination of parasitic resistance and inductance, elimination of added thermal resistance and internal package mechanical stress, space reduction and overall cost reduction.

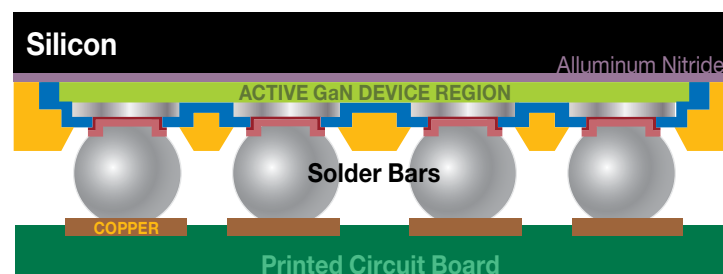


Figure 7: eGa_N™ transistors can be used as a “flip chip”. When compared to plastic packages, this design reduces cost and requires less space.

Even though the devices are not in a “normal” plastic package, it has been demonstrated that they can perform reliably. Fifty EPC1010 transistors were subjected to a drain-source bias of 100 V at 85°C in a humidity chamber with 85% relative humidity (twenty five out of the fifty parts were underfilled). The drain-source leakage, shown in Figure 8, over 1000 hours of stress demonstrates the device stability. As with EPC1010, no drain-source leakage degradation was observed over a 1000 hours stress period for the 40 V (EPC1014 and EPC1015) transistors.

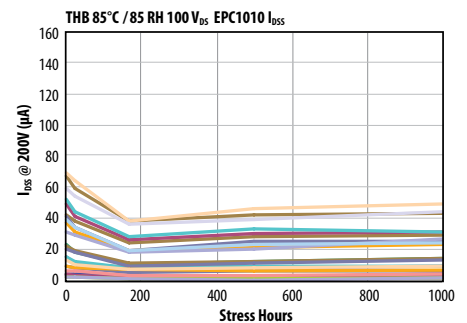


Figure 8. EPC1010 devices were stressed with 100 V applied on the drain at 85°C in a humidity chamber of 85% relative humidity. The drain leakage was measured with 200 V on the drain with gate and source shorted to ground at 25°C.

Moisture Sensitivity Level

EPC's eGa_N transistors are proven MSL1 capable (moisture sensitivity level 1). Fifty EPC1001 dies were stressed following IPC/JEDEC J-STD-202D standard. They were moisture soaked under 85°C and 85% RH for a period of 168 hours, and were then subjected to three cycles of reflow conditions. Parts were electrically tested before and after the stress test, and all parts passed electrical testing post the stress test.

Temperature Cycling

Figure 7 shows how EPC's eGa_N transistor can be used as a “flip chip” mounted onto a printed circuit board (PCB). To test the solder joint stability under temperature cycling for

this configuration, EPC put three device types (EPC1001, EPC1014, EPC1012) under temperature cycling between -40°C to 125°C , at a rate of two cycles per hour. The solder material for these part numbers was eutectic SnPb solder ($63\text{Sn}-37\text{Pb}$)²³ (lead free parts will be introduced in late 2010).

The normalized $R_{\text{DS(on)}}$ was plotted in Figure 9 to show the device stability under this stress condition. The on-state resistance, as well as all other device parameters, stayed stable over the stress period of 1000 cycles.

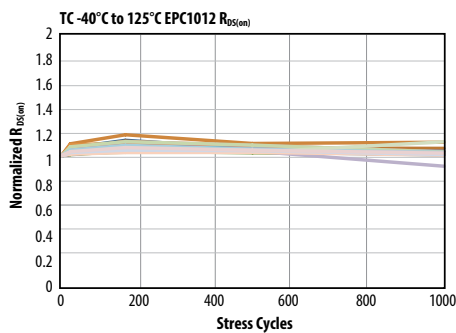


Figure 9. EPC1012 devices were temperature cycled between -40°C and 125°C at a rate of two cycles per hour. $R_{\text{DS(on)}}$ was measured with 5 V on the gate at 25°C .

Device ESD Capability

Electrostatic Discharge (ESD) tests were conducted on EPC1014 and EPC1015. EPC1014 is a smaller size device (1.7 mm x 1.1 mm) and EPC1015 is a larger device (4.1 mm x 1.6 mm) representing the spectrum of EPC's product offerings. Both HBM (human body model) and MM (machine model) tests were conducted on these two part numbers. JESD22-A114F was followed for the HBM, and EIA/JE522-A115-A was followed for the MM. The ESD results are summarized in Table II.

The source-drain has low sensitivity to ESD. On HBM, both EPC1014 and EPC1015 exceeded ± 4000 volt drain-source without fail, making them Class 3A (or higher) capable. On MM both EPC1014 and EPC1015 passed ± 400 volt drain-source, making them Class C capable.

Due to the extremely low input capacitance of EPC's transistors, the gates are ESD sensitive. Both EPC1014 and EPC1015 were Class 1A rated gate-source on HBM and Class A rated gate-source on MM. EPC1015 passed ± 500 volts gate-drain, making it Class 1B capable on HBM, and passed ± 200 volt gate-drain, making it Class B capable on MM. EPC1014 was Class 1A rated gate-drain on HBM and Class A rated gate-drain on MM.

Conclusions

EPC's eGaN transistors bring designers significant performance and size advantages over silicon power MOSFETs. These advantages can be used to improve system efficiency, reduce system cost, reduce size, or a combination of all three. Because EPC's products were designed as power MOSFET replacements, designers can use their existing building blocks, skills and knowledge with only minor changes. Reliability testing has also demonstrated that the technology is now ready for general commercial use.

References

1. S. Singhal, T. Li, A. Chaudhari, A.W. Hanson, R. Therrien, J.W. Johnson, W. Nagy, J. Marquart, P. Rajagopal, J.C. Roberts, E.L. Piner, I.C. Kizilyalli, K.J. Linthicum, "Reliability of Large Periphery GaN-on-Si HFETs," *Microelectronics Reliability* 46, 2006, pp. 1247-1253.
2. S. Singhal, A.W. Hanson, A. Choudhary, P. Rajagopal, T. Li, J.W. Johnson, W. Nagy, R. Therrien, C. Park, A.P. Edwards, E.L. Piner, K.J. Linthicum, I.C. Kizilyalli, "Qualification and Reliability of a GaN Process Platform," <http://www.nitronix.com>.
3. P. Saunier, C. Lee, A. Galisteri, D. Dumka, J. Jimenez, H.Q. Tserng, M.Y. Kao, P.C. Chao, K. Chu, A. Souzis, I. Eliashevich, S. Guo, J. del Alamo, J. Joh, M. Shur, "Progress in GaN Performances and Reliability," in *Proc. Device Res. Conf.*, 2007, pp. 35-36.
4. M. Briere, "GaN on Si Based Power Devices: An Opportunity to Significantly to Impact Global Energy Consumption," *CS MANTECH*, May, 2010.
5. <http://epc-co.com/epc/Products/eGaNfetsandCs.aspx>
6. W. Saito, T. Nitta, Y. Kakiuchi, Y. Saito, K. Tsuda, I. Omura, and M. Yamaguchi, "On-Resistance Modulation of High Voltage GaN HEMT on Sapphire Substrate Under High Applied Voltage," *IEEE Electron Device Letters*, vol. 28, no. 8, 2007, pp. 676-678.
7. R. Veturly, N.Q. Zhang, S. Keller, U.K. Mishra, "The Impact of Surface States on the DC and RF Characteristics of AlGaIn/GaN HFETs," *IEEE Transactions on Electron Devices*, vol. 48, no. 3, 2001, pp. 560-566.
8. J. Joh, and J.A. del Alamo, "Mechanism for Electrical Degradation of GaN High-Electron Mobility Transistors," in *IEDM Tchn. Dig.*, 2006, pp. 415-418.
9. S.Y. Park, C. Floresca, U. Chowdhury, J.L. Jimenez, C. Lee, E. Beam, P. Saunier, T. Balistreri, M.J. Kim, "Physical Degradation of GaN HEMT Devices Under Drain Bias Reliability Testing," *Microelectronics Reliability*, vol. 49, 2009, pp. 478-483.
10. M.A. Mastro, J.R. LaRoche, N.D. Bassim, C.R. Eddy Jr., "Simulation on the effect of non-uniform strain from the passivation layer on AlGaIn/GaN HEMT," *Microelectronic Journal* 36 (2005) 705-711.
11. D. Marcon, A. Lorenz, J. Derluyn, J. Das, F. Medjoud, K. Cheng, S. Degroote, M. Leys, R. Mertens, M. Germain, and G. Borghs, "GaN-on-Si HEMT stress under high electric field condition," *Phys. Status Solidi C*, vol. 6, 2009, pp. S1024-S1028.
12. L. Ma, Y. Wang, T.Y. Guo, J. Lu, Z.B. Hao, Y. Luo, and Z.P. Yu, "Trap Related Current Collapse Effects in GaN HEMTs," *IEEE Conf. on Electron Devices and Solid State Circuits*, 2005, pp. 795-798.
13. T. Mizutani, Y. Ohno, M. Akita, S. Kishimoto, and K. Maezawa, "A Study on Current Collapse in AlGaIn/GaN HEMTs Induced by Bias Stress," *IEEE Transactions on Electron Devices*, Vol. 50, No. 10, 2003, pp. 2015-2020.
14. L. Shen, S. Heikman, B. Moran, et al., "AlGaIn/AlN/GaN High-Power Microwave HEMT," *IEEE Electron Device Letters*, vol. 22, 2001, pp.457-459.
15. Y.C. Chou, D. Leung, I. Smorchkova, M. Wojtowicz, R. Grundbacher, L. Callejo, Q. Kan, R. Lai, P.H. Liu, D. Eng, A. Oki, "Degradation of AlGaIn/GaN HEMTs Under Elevated Temperature Life testing," *Microelectronics Reliability*, vol. 44, 2004, pp. 1033-1038.
16. N. Shgaier, M. Trabelsi, N. Yacoubi, J.M. Bluet, A. Souifi, G. Guillot, C. Gaquiere, J.C. DeJaeger, "Traps Centers and Deep Defects Contribution in Current Instabilities for AlGaIn/GaN HEMT's on Silicon and Sapphire Substrates," *Microelectronics Journal* 37, 2006, pp. 363-370.
17. G. Meneghesso, G. Verellesi, F. Danesin, F. Rampazzo, F. Zanon, A. Tazzoli, M. Meneghini, and E. Zanoni, "Reliability of GaN high-electron-mobility transistors: state of the art and perspectives," *IEEE Transactions on Device and Materials Reliability*, vol. 8, no. 2, 2008, pp. 332-343.
18. J. Joh, L. Xia, and J.A. del Alamo, "Gate Current Degradation Mechanisms of GaN High Electron Mobility Transistors," in *IEDM Tech. Dig.*, 2007, pp. 385-388.
19. J.L. Jimenez, U. Chowdhury, "X-Band GaN FET Reliability," *Reliability Physics Symposium, IEEE International*, April 2008, pp. 429-435.
20. D. Kumar Sahoo, R.K. Lal, H. Kim, V. Tilak, and L.F. Eastman, "High-Field Effects in Silicon Nitride Passivated GaN MODEFTs," *IEEE Transactions on Electron Devices*, vol. 50, no. 5, 2003, pp. 1163-1170.
21. S. Singhal, J.C. Roberts, P. Rajagopal, T. Li, A.W. Hanson, R. Therrien, J.W. Johnson, I.C. Kizilyalli, K.J. Linthicum, "GaN-on-Si Failure Mechanisms and Reliability Improvements," in *Proc. IEEE Int. Rel. Phys. Symp.*, 2006, pp. 95-98.
22. Y. Ma, "EPC GaN Transistor Application Readiness," http://epc-co.com/epc/documents/product-training/EPC_relreport_030510_finalfinal.pdf
23. A. Nakata, E. Abdoulin, J. Cao, Y. Ma, "Assembling GaN Transistors," http://epc-co.com/epc/documents/product-training/Appnote_GaNAssembly.pdf

Table I: EPC eGaN Transistor Reliability Results Overview

Stress Test	Test Condition	Part Number	Sample Size	# of Fails	
				1000 HR	3000 HR
HTRB	100 V _{DS} , 125°C	EPC1001	45	0	–
HTRB	40 V _{DS} , 125°C	EPC1014	50	0	–
HTRB	200 V _{DS} , 125°C	EPC1012	50	0	–
HTRB	200 V _{DS} , 125°C	EPC1010 with underfill	50	0	–
HTRB	200 V _{DS} , 150°C	EPC1010	50	0	0
Stress Test	Test Condition	Part Number	Sample Size	# of Fails	
				1000 HR	3000 HR
HTGB 5 V	5 V _{GS} , 125°C	EPC1001	45	0	0
HTGB 5.4 V	5.4 V _{GS} , 125°C	EPC1001	45	0	0
HTGB 5 V	5 V _{GS} , 150°C	EPC1010	45	0	–
HTGB -5 V	-5 V _{GS} , 125°C	EPC1001	50	0	–
Stress Test	Test Condition	Part Number	Sample Size	# of Fails	
				1000 cys	
TC	-40°C to 125°C	EPC1001	45	0	-
		EPC1014	50	0	-
		EPC1012	45	0	-
		EPC1012 with underfill	45	0	-
Stress Test	Test Condition	Part Number	Sample Size	# of Fails	
				1000 HR	
THB	85C/85 RH, 40 V _{DS}	EPC1014	45	0	-
THB	85C/85 RH, 40 V _{DS}	EPC1015	45	0	-
THB	85C/85 RH, 100 V _{DS}	EPC1010	25	0	-
THB	85C/85 RH, 100 V _{DS}	EPC1010 with underfill	25	0	-
Stress Test	Test Condition	Part Number	Sample Size	# of Fails	
				168 HR	
MSL1	85C/85 RH, 168 HR	EPC1001	50	0	-
Stress Test	Test Condition	Part Number	Sample Size	# of Fails	
				1200 HR	
Power Supply Life Test	10 A, 250 kHz, 30C	EPC1001	10	0	-

Table II: ESD Results

Pin-Pin(+/-)	EPC1015 HBM	EPC1014 HBM	EPC1015 MM	EPC1014 MM
G-S (+)	CLASS 1A	CLASS 1A	CLASS A	CLASS A
G-S (-)	CLASS 1A	CLASS 1A	CLASS A	CLASS A
G-D (+)	CLASS 1B	CLASS 1A	CLASS B	CLASS A
G-D (-)	CLASS 1B	CLASS 1A	CLASS B	CLASS A
S-D (+)	> CLASS 3A	> CLASS 3A	CLASS C	CLASS C
S-D (-)	> CLASS 3A	> CLASS 3A	CLASS C	CLASS C